

## Fluid dynamics of the resonance tube

By E. BROCHER, C. MARESCA AND M.-H. BOURNAY

Institut de Mécanique des Fluides de l'Université  
d'Aix-Marseille, Marseille, France

(Received 2 December 1969)

Using a simplified wave-diagram and the gas-speed/sound-speed diagram, it is shown how the oscillations start and grow within a resonance tube. It is found that the oscillation amplitude tends to a limiting value which is obtained when the jet is fully swallowed by the tube during the phase of compression of the cycle. Experiments are carried out for jet Mach numbers from 0.1 up to 2. To achieve an adequate evacuation of the tube in the expansion phase, a thin cylindrical body must be used, which is laid along the axis of the jet to produce a wake and a correlative local deficiency of the kinetic energy of the jet. Measured amplitudes of pressure fluctuations are in good agreement with theoretical values.

---

### 1. Introduction

Hartmann (1919) has discovered that strong oscillations can be produced in a cavity facing a supersonic under-expanded jet. He found that oscillations only occur when the cavity mouth is placed at certain locations of the periodic structure of the jet. Since then, numerous investigators have studied this interesting unsteady flow phenomenon.

It was found by Savory (1950) and Hartmann & Trudso (1951) that, when the resonator cavity is supported by a stem passing through the nozzle and lying along its axis, oscillations may still occur when the jet is slightly subsonic. Sprenger (1954) was able to obtain an oscillating flow with jet Mach numbers as low as 0.52 by placing a thin nylon thread ( $10^{-3}$  cm diameter) across the jet axis. Vrebalovich (1962) observed oscillations in a cavity placed in a subsonic or supersonic flow field by putting a ring trip or a wing trip upstream of the tube mouth.

Brocher & Maresca (1969*a*) suggested that the main condition to obtain flow oscillations within a cavity facing a subsonic jet or exposed in a subsonic gas flow, is to decrease the energy of the jet in the neighbourhood of its axis in order to act upon the radial pressure distribution at the cavity entrance. This is confirmed by experiments carried out with a thin cylinder placed axially in the jet nozzle which produces a wake in the centre of the jet. The same authors (1969*b*) were also able to predict both the maximum amplitude and the frequency of the oscillations for low jet Mach numbers. Brocher, Maresca & Husson (1969) extended the analysis to higher subsonic jet Mach numbers and good agreement was found between theory and experiments.

The purpose of the present paper is to review the most important results already achieved by the authors, also to extend the analysis to the case of a supersonic correctly expanded jet, and to estimate the effect of the increase in temperature of the tube (Sprenger 1954) on the oscillation amplitude. Also the need for decreasing the energy of the jet on its axis to initiate and sustain the oscillation will be clearly demonstrated in the gas-speed/sound-speed diagram. It is shown experimentally that the 'wake-producing' cylinder, laid down along the jet axis, achieves oscillation amplitudes that are in good agreement with the theoretical predictions over the whole range of jet Mach numbers tested (0.1–2.0).

## 2. Oscillations mechanism

For the investigation of unsteady flows, it is customary to use two diagrams: (a) the wave diagram; (b) the gas-speed/sound-speed diagram.

Most of the previous investigators have represented the wave processes of the resonance tube, using the wave diagram only. Others, such as Thompson (1964) and Manning (1968) recognized the interest of representing the processes in the second diagram. The authors (1969) have shown that the latter enables one to demonstrate how the oscillation may start and grow to a definite limiting value.

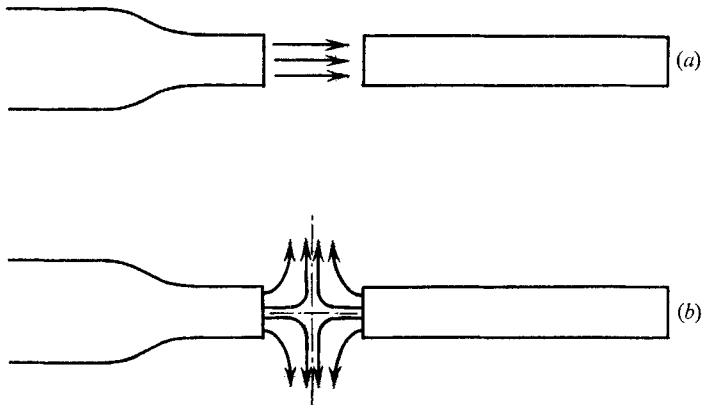


FIGURE 1. Flow phases in a resonance tube. (a) First phase: penetration of the jet into the tube. (b) Second phase: evacuation of the tube.

First, it should be recalled that the flow in a resonance tube may be divided into two phases; in the first phase, the jet penetrates into the tube and compresses the gas contained therein; in the second phase, the gas compressed in the tube expands to the atmosphere and the jet is deviated laterally (figure 1). A simplified wave diagram of the process in the resonance tube is represented in figure 2. It consists essentially in a compression wave, a reflected compression wave, an expansion wave and a reflected expansion wave. Also shown in the figure is the entropy line or contact front, between the gas of the jet and the gas contained in the cavity. The following simplifications are made to investigate the mechanism of the oscillations:

(i) Viscous effects are neglected. This approximation is good when the

Reynolds number based on the tube diameter and on the jet velocity, is sufficiently high and/or when the tube length/tube diameter ratio is not too large.

(ii) Compression waves are considered as isentropic. This hypothesis is good for jet Mach numbers  $M_j$ , up to about 1. For higher jet Mach numbers, it is also applicable if the compression waves do not have time to coalesce to form a shock wave, that is, for relatively small tube length.

(iii) Wave reflexions on the contact front are neglected. This approximation is good for  $M_j$  up to about 1.3, if the tube is cooled to compensate for the heating effects due to irreversibilities.

(iv) Wave bundles are replaced by single waves. For the wave diagram and the detailed configuration of the oscillations, this is a rather crude approximation. But, to describe the phenomena, it is a very convenient simplification and it turns out to give fairly accurate results for the oscillation amplitude.

(v) The flow in the jet is quasi-steady. As indicated above, the flow in a resonance tube comprises essentially two phases: a compression phase and an expansion phase. The flow in the jet may be considered as steady, during each of these phases, if the switching time from one phase to the other is short compared to the period of oscillation. This condition will be met when the length/diameter ratio of the tube is sufficiently large.

With these hypotheses, it is possible to describe quite clearly in the gas-speed/sound-speed diagram how the oscillations start and grow in the resonance tube.

The flow in the jet being considered as quasi-steady, the conservation of energy may be written as

$$a_3^2 + \frac{\gamma-1}{2} u_3^2 = a_0^2, \tag{1}$$

where  $a_3$  and  $u_3$  are respectively the sound speed and the gas speed in the jet penetrating into the tube (region 3 of figure 2),  $a_0$  the stagnation-point sound speed of the jet and  $\gamma$  the specific heat ratio. Equation (1) represents an ellipse in the  $a, u$  plane and may be called 'ellipse of energy'.

In the resonance tube the flow is unsteady. Since it is considered as isentropic, the Riemann invariants

$$\frac{2}{\gamma-1} a \pm u = \text{constant} \tag{2}$$

may be used. In the  $a, u$  plane, (2) represents straight lines, the slopes of which are

$$\frac{da}{du} = \mp \frac{\gamma-1}{2}. \tag{3}$$

In order to simplify the drawing, it is convenient to introduce the following non-dimensional co-ordinates

$$U \equiv \frac{\gamma-1}{2} \frac{u}{a_0},$$

$$A \equiv \frac{a}{a_0}.$$

In the  $A, U$  plane, (1) becomes

$$A_3^2 + \frac{2}{\gamma-1} U_3^2 = 1, \tag{4}$$

which is again an ellipse, and (2) becomes

$$A \pm U = \text{constant}, \quad (5)$$

which is the equation of straight lines, the slopes of which are  $\mp 1$ . It may be shown that there exists a simple relation between the speed of sound of the jet

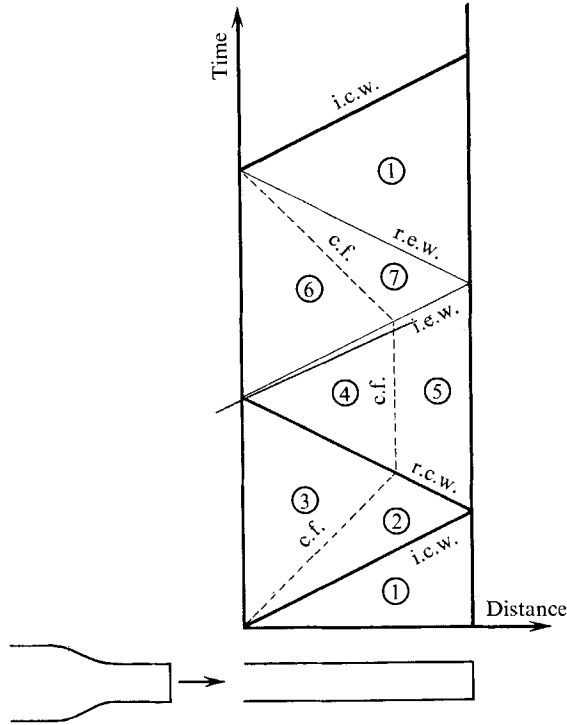


FIGURE 2. Wave diagram of the resonance tube. i.c.w., incident compression wave; r.c.w., reflected compression wave; i.e.w., incident expansion wave; r.e.w., reflected expansion wave; c.f., contact front.

penetrating into the tube and that of the gas on the other side of the contact front (region 2 in figure 2). Since the flow in the jet is isentropic, one has, at any cycle  $n$ ,

$$\frac{a_{3n}}{a_0} = \left( \frac{p_{3n}}{p_0} \right)^{(\gamma-1)/2\gamma}, \quad (6)$$

where  $a_{3n}$  and  $p_{3n}$  are respectively the pressure and the sound speed in the region 3 and  $p_0$  is the total pressure of the jet. If the flow is isentropic, one has for the sound speed in region 2, after any number  $n$  of cycles

$$\frac{a_{2n}}{a_{20}} = \left( \frac{p_{2n}}{p_{20}} \right)^{(\gamma-1)/2\gamma}, \quad (7)$$

where  $a_{20}$  and  $p_{20}$  are respectively the speed of sound and the pressure of the gas filling the cavity before the oscillations start. For  $a_{20}$  and  $p_{20}$  the following remarks apply. In most cases  $p_{20}$  will be equal to the surrounding pressure. Moreover, it is known (Sprenger 1954) that thermal effects occur in resonance tubes. This is due

to the friction on the walls and to irreversibilities in shocks. Indeed, although the irreversible heat produced at each cycle may be small compared to the energy of the jet, the cumulative effect of such irreversibilities may be important. It is experimentally observed that the temperature of the tube increases and levels off to some value. The thermal effects grow as the jet Mach number increases. To take them into account it will be here assumed that the flow is isentropic at each cycle but that the temperature level of the cavity may be higher than the surrounding temperature. In other words, it is assumed that the tube has been heated up at its final equilibrium temperature before the oscillations start; with this assumption,  $a_{2_0}$  in (7) will be the speed of sound of the gas at a suitable mean temperature of the tube walls.

The speeds of sound  $a_{2n}$  and  $a_{3n}$  are then related by

$$\begin{aligned} \frac{a_{2n}^2}{a_{3n}^2} &= \frac{a_{2_0}^2 (a_{2n}/a_{2_0})^2}{a_0^2 (a_{3n}/a_0)^2} \\ &= \frac{T_{2_0} (p_{2n}/p_{2_0})^{(\gamma-1)/\gamma}}{T_0 (p_{3n}/p_0)^{(\gamma-1)/\gamma}}. \end{aligned}$$

Noting that  $p_{2n} = p_{3n}$  across the contact front, then

$$\frac{A_{2n}^2}{A_{3n}^2} = \alpha^{-1} \pi^{(\gamma-1)/\gamma}, \tag{8}$$

where  $\alpha$  is the temperature ratio  $T_0/T_{2_0}$ . If no thermal effect were present and the total temperature of the jet were equal to the ambient temperature,  $\alpha$  would be equal to unity.  $\pi$  is the pressure ratio  $p_0/p_{2_0}$  of the jet and determines the jet Mach number. Combining (4) and (8) and noting that  $U_{3n} = U_{2n}$  across the contact front, we obtain

$$\alpha \pi^{-(\gamma-1)/\gamma} A_{2n}^2 + \frac{2}{\gamma-1} U_{2n}^2 = 1. \tag{9}$$

Hence, in the  $A, U$  plane, the flow conditions in region 2 of figure 2 are located on the ellipse  $E_2$  given by (9), which is a similar transformation of the energy-ellipse of the jet  $E_3$ . It is now possible to describe how the oscillations start and may grow in a resonance tube. Let it be supposed that the mouth of the tube is closed by a plate. The flow configuration will then be that of stagnation point flow on a plate with its centre on the axis of the jet. Hence, the pressure around the axis will be higher than the surrounding pressure. If the plate is suddenly removed, the jet will produce a compression wave in the tube which was filled with gas at the surrounding pressure. In the  $A, U$  plane (figure 3), this compression wave, considered as isentropic, goes from the point  $1^1$  ( $U = 0; A_{2_0} = \alpha^{-\frac{1}{2}}$ ), with the slope  $+1$ ; the intersection point  $2^1$  of this wave with the ellipse  $E_2$  gives the flow conditions in the region 2 during the first cycle. The flow conditions of the jet penetrating the cavity are given by the point  $3^1$ .

The compression wave is then reflected by the end wall of the tube. This reflected wave is represented by two straight lines with slope  $-1$ , one starting from point  $2^1$  for the gas that was initially in the tube and the other from point  $3^1$ , for the gas of the jet that penetrated into the tube. The boundary condition at

the wall being  $U = 0$ , the flow conditions in regions 4 and 5 are given by the intersection of these lines with the axis  $U = 0$  (points  $4^1$  and  $5^1$ ). When the reflected compression wave reaches the tube mouth, it pushes the jet backwards and by doing so, it allows the tube to empty. The compression wave will be reflected as an expansion wave at the mouth. This expansion wave is a straight line with slope  $+1$ . The crucial point is now to determine how far down the pressure will decrease behind this wave. Obviously, the gas coming out of the cavity has to

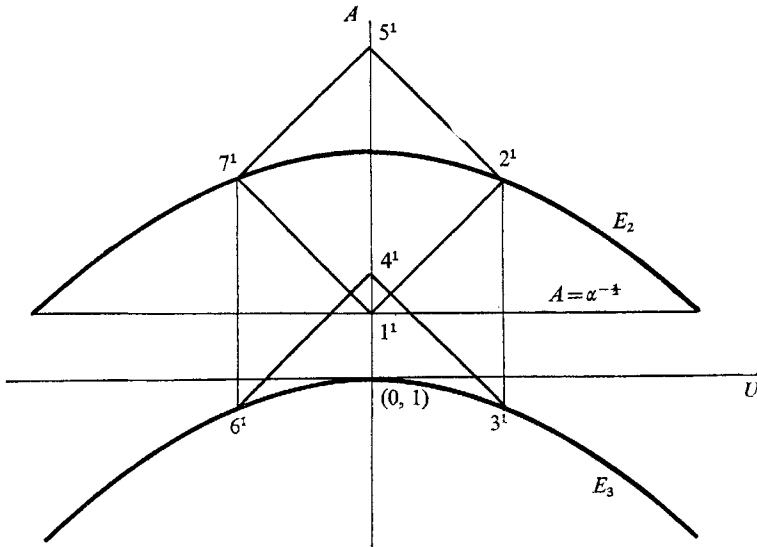


FIGURE 3. Gas-speed/sound-speed diagram ( $U \equiv \frac{1}{2}(\gamma-1)u/a_0$ ,  $A \equiv a/a_0$ ).  $E_3$ , energy-ellipse of the jet;  $E_2$ , locus of flow conditions in region 2.

have a total pressure at least equal to the total head of the jet in order to push it backwards. At the point  $4^1$ , the total head of the gas is higher than that of the jet but the unsteady expansion reduces this total head. It is easy to see that when this gas has been brought to the state  $6^1$ , its total head will just be equal to the total head of the jet; indeed at point  $6^1$  the static pressure and the Mach number are the same as at point  $3^1$  which is on the energy ellipse  $E^3$ . Hence the expansion wave will bring the gas coming out of the cavity to the point  $6^1$ . The corresponding state of the gas contained initially in the tube will be given by the point  $7^1$  and the reflected expansion wave will bring this gas back to the starting point  $1^1$ . It follows that the cycle will repeat itself and that the amplitude of the pressure fluctuations will remain constant with time. In experiments of course, friction and other irreversibilities will act as a damping force and the pressure fluctuations will die out as indicated schematically on figure 4. The final conditions in the tube will be given by the intersection of ellipse  $E_2$  with the axis  $U = 0$ , that is, the tube will be filled at a pressure equal to the total head of the jet. In order to amplify the fluctuations, it is therefore necessary to have some mean to help the tube emptying to a lower pressure.

During the expansion phase of the cycle the flow configuration is that of two jets with the same total head (neglecting viscous losses) flowing coaxially against

each other. If, as was proposed by Brocher & Maresca (1969*a, b*), a cylindrical rod is inserted along the axis of the jet nozzle, the total head of the jet coming out of the nozzle will be reduced around the axis and, in this region, will be smaller than the total head of the flow coming out of the tube. Consequently, this flow will be able to push the jet farther back, especially around the axis. In order to investigate the effect of a rod on the pressure distribution at the entrance of the tube, experiments have been carried out with the entrance of the tube closed by a plate. The measured pressure distributions on the plate with and without a rod are shown on figure 5. It is seen that a thin cylinder is sufficient to modify the pressure distribution in a region much wider than the cylinder diameter.

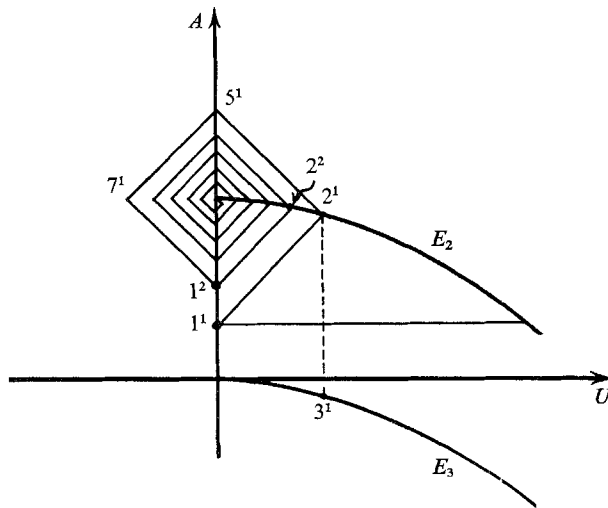


FIGURE 4. Case of insufficient evacuation of the tube: the oscillations damp out.

Hence a thin cylinder is sufficient to greatly help the flow coming out of the tube push back the jet. The expansion wave will then bring the pressure in the tube to a lower level than that corresponding to the points  $6^1$  and  $7^1$  of figure 3. In fact, if the jet is pushed back sufficiently far, the flow coming out of the tube is that of a free jet and its static pressure is atmospheric. It may therefore be assumed that the expansion wave brings the gas to ambient pressure (figure 6). In that case, the expansion wave starting from point  $5^1$  with slope  $+1$  will reach the horizontal line  $A = \alpha^{-\frac{1}{2}}$  and the point  $7^1$  will be located at the intersection with this line. The expansion wave will be reflected by the end wall of the tube as another expansion wave; this wave will bring the gas to rest, that is, to the point  $1^2$ . At this point the pressure is below the ambient pressure and there is a suction effect in the tube. The compression wave of the second cycle will be stronger than that of the first cycle, and will bring the gas to the point  $2^2$ . After the passage of the reflected compression wave, the gas will be in the state  $3^2$ , and so on. It is seen that the oscillation amplitude will grow up at each cycle. As is demonstrated in the appendix, the oscillation will tend to the cycle  $1-2-5-7-1$  as the number of cycles tends to infinity. Hence, even in the absence of losses the oscillation amplitude does not become infinite but grows only to a definite

limiting value. It is therefore appropriate to call the cycle 1-2-5-7-1 the 'limit cycle'.

It is seen from figure 6 that the speed of sound  $A_{2^n}$  behind the incident shock decreases at each cycle and tends to the limit value  $A_{2_0}$ . From (7), it follows that the pressure behind the incident shock will decrease at each cycle until it is just

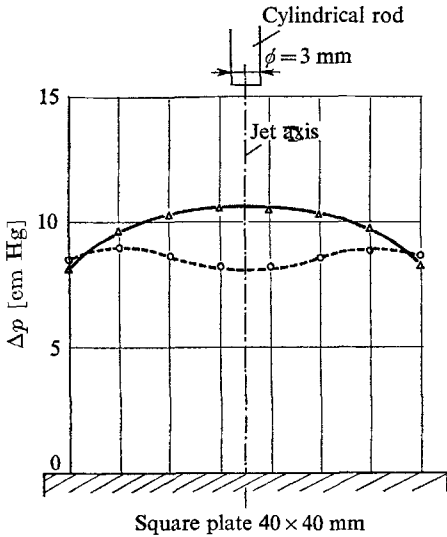


FIGURE 5

FIGURE 5. Jet impinging on a plate: pressure distribution on the plate without and with 'wake-producing' rod. Squared jet 36 × 36 mm. Jet Mach number: 0.44. Δ: without rod; ○: with rod.

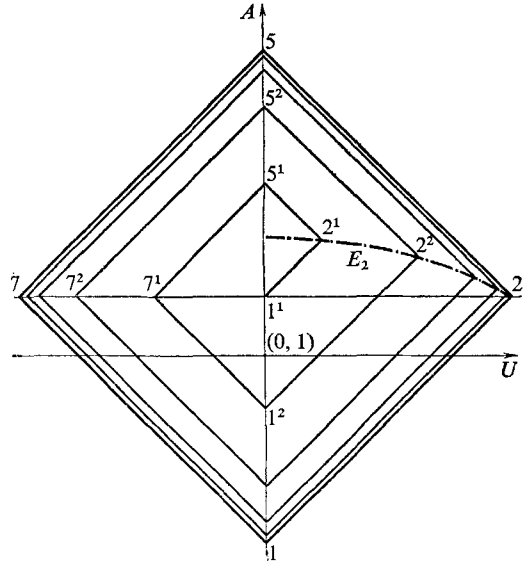


FIGURE 6

FIGURE 6. Case of evacuation down to surrounding pressure: the oscillations grow up until full resonance is reached.

equal to the surrounding pressure  $p_{2_0}$ . Hence, during the starting process of a resonance tube, the tube will gradually empty itself. When the limit cycle is reached, the pressure ahead of the incident shock is below atmospheric and is exactly such that the jet can be fully swallowed by the tube in the compression phase of the cycle.

It should finally be noted that the 'wake-producing' device is not only necessary during the starting and the growing of the oscillations but also when the limit cycle is reached. Indeed, in experiments, the total head of the flow coming out of the tube is reduced by irreversibilities (friction, shocks) and the total head of the jet has to be decreased in its centre to help the tube emptying, as discussed above. This is experimentally confirmed by removing the wake-producing device after the limit cycle has been reached: the oscillations immediately damp out.

### 3. Limit cycle

No distinction has been made between subsonic and supersonic jet velocities in the description of the starting and growing of the oscillations in a resonance tube. It will be seen below that the limit cycle described so far applies, strictly



speaking, to subsonic jet velocities only. However, experimental evidence will show that certain features of this cycle remain valid for a correctly expanded supersonic jet.

(a) Subsonic jet

Since the point 2 is given by the intersection of the horizontal line  $A = A_{2_0}$  and the ellipse  $E_2$  (equation (9)), the gas velocity at point 2 is given by

$$U_2 = [\frac{1}{2}(\gamma - 1)(1 - \pi^{-(\gamma-1)/\gamma})]^{\frac{1}{2}} \tag{10}$$

The pressure at point 2 is equal to atmospheric pressure. Since the pressure is the same on both sides at the contact front, one sees that when the limit cycle is reached, the static pressure of the jet penetrating in the tube is equal to atmospheric pressure. Therefore, the speed of the jet penetrating the tube is the same as the speed of the jet discharging in the atmosphere and the jet may penetrate completely into the tube during the compression phase of the cycle. The pressure ratio appearing in (10) may be expressed in terms of the jet Mach number  $M_j$ :

$$\pi^{(\gamma-1)/\gamma} = 1 + \frac{1}{2}(\gamma - 1)M_j^2$$

and the points of the limit cycle are then given by

$$\left. \begin{aligned} 2: U_2 &= \frac{\frac{1}{2}(\gamma - 1)M_j}{[1 + \frac{1}{2}(\gamma - 1)M_j^2]^{\frac{1}{2}}}; & A_2 &= A_{2_0} = \alpha^{-\frac{1}{2}}. \\ 5: U_5 &= 0; & A_5 &= A_{2_0} + U_2. \\ 7: U_7 &= -U_2; & A_7 &= A_{2_0} = \alpha^{-\frac{1}{2}}. \\ 1: U_1 &= 0; & A_1 &= A_{2_0} - U_2. \end{aligned} \right\} \tag{11}$$

It is now easy to calculate the variation of other physical quantities once the limit cycle is reached. For instance, the pressure at the points 5 and 1 is given by

$$\frac{p_5}{p_{2_0}} = \left(\frac{A_5}{A_{2_0}}\right)^{2\gamma/(\gamma-1)} = \left\{1 + \alpha^{\frac{1}{2}} \frac{\frac{1}{2}(\gamma - 1)M_j}{[1 + \frac{1}{2}(\gamma - 1)M_j^2]^{\frac{1}{2}}}\right\}^{2\gamma/(\gamma-1)} \tag{12}$$

$$\frac{p_1}{p_{2_0}} = \left(\frac{A_1}{A_{2_0}}\right)^{2\gamma/(\gamma-1)} = \left\{1 - \alpha^{\frac{1}{2}} \frac{\frac{1}{2}(\gamma - 1)M_j}{[1 + \frac{1}{2}(\gamma - 1)M_j^2]^{\frac{1}{2}}}\right\}^{2\gamma/(\gamma-1)} \tag{13}$$

For  $\alpha = 1$ , (12) and (13) reduce to those previously given by the authors (1969). Since the friction on the walls and the shock irreversibilities heat up the tube,  $\alpha$  will, in general, be smaller than unity. It follows that, according to the simplified model presented here, the heating of the tube will tend to decrease the pressure amplitude since  $p_5/p_{2_0}$  will be smaller and  $p_1/p_{2_0}$  larger. It will now be shown that (11), (12) and (13) are valid for  $M_j \leq 1$ , only. Indeed, in the expansion phase  $M_6 \leq 1$  since the last expansion wave of the expansion bundle gives the condition  $|u_6| \leq a_6$ . One has the relation

$$M_7 = \frac{|u_7|}{a_7} = M_6 \frac{a_6}{a_7}.$$

Since the waves are supposed to be isentropic,  $a_6/a_7 = a_3/a_2$ . Using (8), we get

$$M_7 = M_6 \alpha^{\frac{1}{2}} \pi^{-(\gamma-1)/2\gamma} \tag{14}$$

$M_7$  may be written in the form

$$M_7 = \frac{2}{\gamma - 1} \frac{|U_7|}{A_7} \tag{15}$$

Combining (14) and (15), and putting the condition  $M_6 \leq 1$ , we obtain

$$\frac{|U_7|}{A_7} \leq \frac{\gamma-1}{2} \alpha^{\frac{1}{2}} \pi^{-\frac{1}{2}(\gamma-1)}. \quad (16)$$

Making use of (11), it is easy to show that the condition (16) can be put in the form

$$\pi \leq [\frac{1}{2}(\gamma+1)]^{\gamma/\gamma-1}.$$

As the right-hand side is just equal to the critical pressure ratio, the analysis is valid for  $M_j \leq 1$  only.

(b) *Supersonic jet*

As has been seen above, the simplified model used so far is applicable to subsonic jets only. For correctly expanded supersonic jets, a new approach, based on some of the theoretical results obtained for the subsonic jet and on experimental evidence, will be followed. The case of a correctly expanded supersonic jet has already been studied by Thompson (1964). According to him, there was always a shock standing in front of the mouth of the resonance tube in his experiments. This means that although the jet was supersonic, the flow inside the tube was fully subsonic. Experimental evidence indicates that the wake-producing cylinder enables a penetration of the tube at supersonic velocities. As may be seen on figure 7, plate 1, which is a picture taken from a high speed motion picture (2000 frames/s), no shock appears in front of the tube and the Mach lines remain visible at the very entrance of the tube. Hence, as was the case for subsonic jets, the jet appears to be fully swallowed by the tube. This means that when the limit cycle is reached, the pressure behind the incident shock must just be equal to the surrounding pressure. This experimental fact will form the basis of the model proposed for supersonic jets. However, instead of considering isentropic waves as was done for the subsonic jet, shock relations will be used for the incident and reflected shocks, since the shock irreversibilities may no longer be neglected. The pressure ratios for the incident and reflected shocks are (Oertel 1966),

$$\frac{p_1}{p_{2_0}} = \frac{1+f}{(2+f)M_s^2-1}, \quad (17)$$

$$\frac{p_5}{p_{2_0}} = \frac{(3+f)M_s^2-2}{M_s^2+1}, \quad (18)$$

where  $f$  is the number of degree of freedom or  $f = 2/(\gamma-1)$ . The shock Mach number  $M_s$  is related to  $M_2$  by

$$M_2 = \frac{f(M_s^2-1)}{(M_s^2+f)^{\frac{1}{2}}[(2+f)M_s^2-1]^{\frac{1}{2}}}. \quad (19)$$

Moreover, for supersonic entrance,  $M_2$  is related to the jet Mach number  $M_j$  by

$$M_2 = M_j[1 + \frac{1}{2}(\gamma-1)M_j^2]^{\frac{1}{2}} \alpha^{\frac{1}{2}}. \quad (20)$$

It is therefore possible to express  $p_1/p_{2_0}$  and  $p_5/p_{2_0}$  as functions of  $M_j$  with  $\alpha$  as a parameter.

As mentioned above, the schlieren pictures indicate that no shock is standing at the entrance of the tube. There are two further pieces of experimental evidence

that this is the case. If there were a shock standing in front of the tube mouth, the flow would be subsonic downstream of this shock and equations (12) and (13) can be used by taking the values of  $M_j$  and  $p_{2_0}$  downstream of it. On figure 8, the theoretical values obtained for supersonic and subsonic entrance are compared with the experimental ones obtained at  $M_j = 1.65$  and 2. The parameter  $\alpha$  has been taken equal to 1, which corresponds to the present experimental conditions. It is seen that the experimental values lie closer to the theoretical value obtained for supersonic entrance.

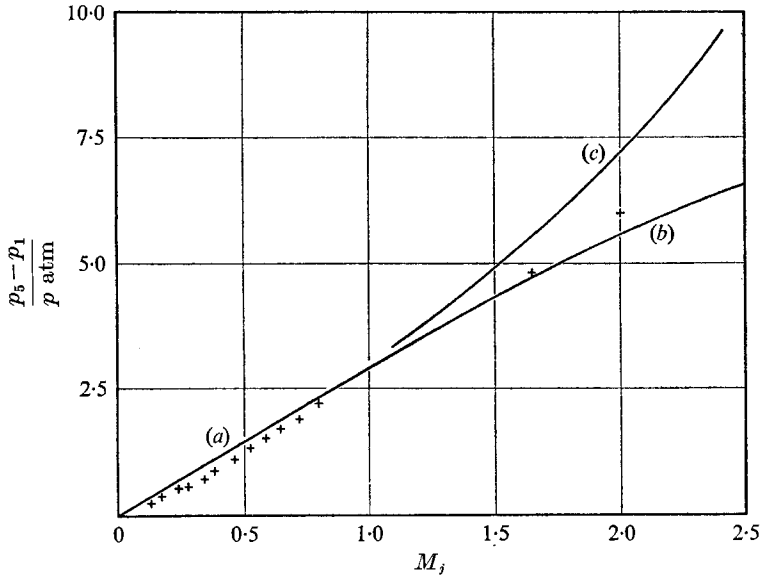


FIGURE 8. Amplitude of pressure fluctuations at the end wall of a resonance tube (with  $\alpha = 1$ ). Curve: (a), subsonic jet; (b), supersonic jet with supersonic entrance into the tube; (c), supersonic jet with subsonic entrance (standing shock in front of the tube mouth).

More experimental evidence of supersonic entrance is the ratio of the reflected shock speed to the incident shock speed. Expressed in terms of the incident shock Mach number  $M_s$  this ratio is equal to (Oertel 1966)

$$\frac{u_{r.s.w.}}{u_{i.s.w.}} = \frac{2(\gamma - 1)M_s^2 + (3 - \gamma)}{(\gamma + 1)M_s^2}.$$

For  $M_s = 1$ , that is for sound waves, this ratio is equal to 1. But as  $M_s$  increases, the ratio decreases since the incident shock velocity is higher than the reflected shock velocity in the laboratory co-ordinates. It should be noted that the ratio is independent of the sound speed of the gas. Hence, it is insensitive to the thermal effects that may occur in the tube.

It is possible to express  $M_s$  as a function of  $M_j$  for the cases of supersonic and subsonic entrance. One may then express the speed ratio as a function of  $M_j$  for the two cases. The result of this computation is given in figure 9 and is compared

with the experimental values obtained for  $M_j = 1.65$  and 2. As may be seen the experimental values lie much closer to the theoretical value obtained for supersonic entrance.

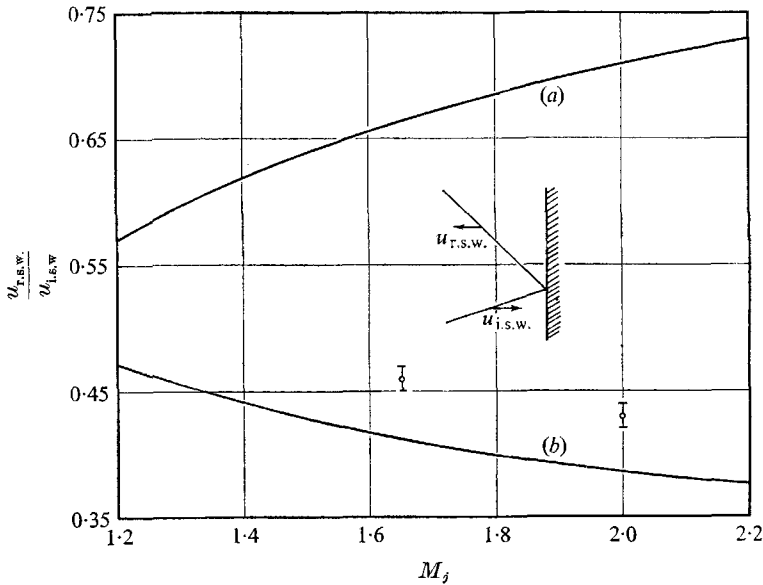


FIGURE 9. Ratio of reflected shock velocity to incident shock velocity. Curve: (a), supersonic entrance into the tube (standing shock); (b), supersonic jet with supersonic entrance into the tube.

#### 4. Experiments

Two interesting results of the theoretical analysis of the limit cycle are that the minimum pressure of the cycle is below the surrounding pressure and that the maximum pressure is above the stagnation pressure of the jet. It is difficult to verify these facts experimentally in a resonance tube working with gas. Indeed, to measure the pressure fluctuation in that case, use is made of piezo quartz and the drift of electronic circuits does not allow a precise measurement of the absolute pressure level. Therefore, experiments have first been carried out on the hydraulic analogue of the resonance tube and the experimental results have confirmed the two theoretical predictions mentioned above (Brocher & Maresca 1969*b*; Brocher, Maresca & Husson 1969).

Experiments have then been carried out with the resonance tube itself. Figure 10 represents the experimental set up. The resonance tube is of prismatic form. In all experiments reported here, the cross-sectional area of the nozzle exit and of the resonance tube are equal (36 mm × 36 mm). A thin rod is placed on the axis of the jet nozzle so as to produce the desired pressure distribution in the jet. For the subsonic velocities, the distance separating the nozzle exit and the tube entrance is equal to the tube width (36 mm). For the supersonic case, this distance is double. Pressure fluctuations have been measured at three locations along the resonance tube: near the mouth, in the middle and at the end wall. The

pressure transducer mounted on the end wall is a Kistler 701 A and the two others are of capacitive type (Dumitrescu 1967). Figure 11 represents two typical records of pressure fluctuations registered on an oscilloscope Tektronix RM 564. One of the hypotheses of the theory is that the wave bundles are replaced by single waves. The corresponding pressure profile would then consist of pressure steps

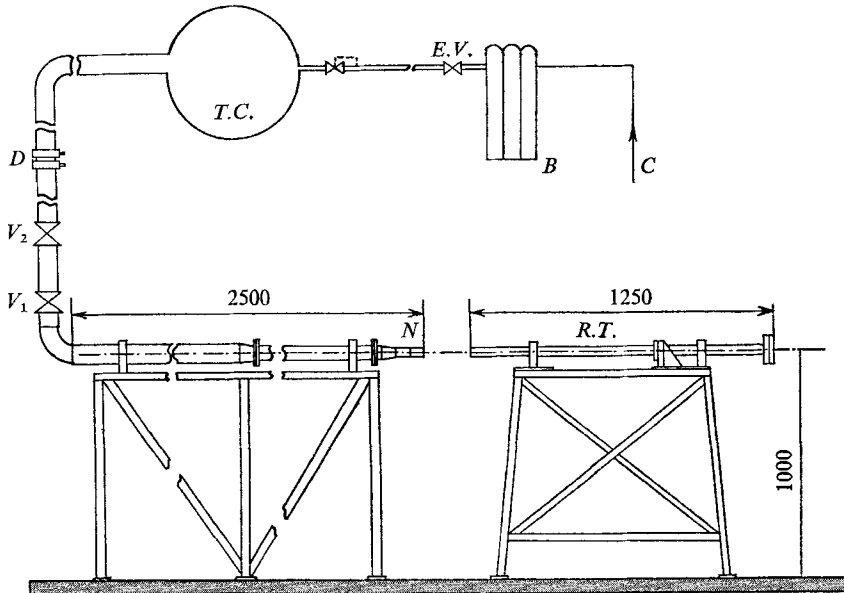


FIGURE 10. Experimental set up. *C*, compressor; *B*, high pressure bottles; *E.V.*, electrovalve; *T.C.*, tranquilization chamber; *D*, diaphragm;  $V_2$ ,  $V_1$ , valves; *N*, nozzle; *R.T.*, resonance tube. Dimensions in (mm).

followed by constant pressure intervals. As may be seen from the records, this is only a very crude picture of the pressure fluctuations. Although the shocks are quite well formed, the expansion waves, as could be expected, give a continuously decreasing pressure. Still, for the subsonic jet velocities, the arrival of the reflected expansion wave may be seen on the trace corresponding to the middle of the tube. At the same location, for supersonic jet velocities, there is a remarkably constant pressure between the arrival of the incident compression wave and its reflexion. At the end wall, for subsonic and supersonic jet velocities, the incident shock and its reflexion are followed by a gradual compression. Near the mouth of the resonance tube, the pressure is more constant in the subsonic than in the supersonic case; but, in both cases, the arrival of the reflected shock gives a very sharp pressure step.

The measured pressure amplitude is plotted in figure 8 and compared with the theoretical predictions of § 3. The agreement is seen to be good over all the range of Mach number tested.

For low jet Mach numbers, the linearized theory (Brocher & Maresca 1969*b*) indicates that the resonance frequency  $\nu$  is independent of  $M_j$  and is equal to the acoustic frequency  $\nu_0 = a_0/4L$  of the tube, that is

$$\nu = \nu_0 \{1 + O(M_j^2)\}.$$

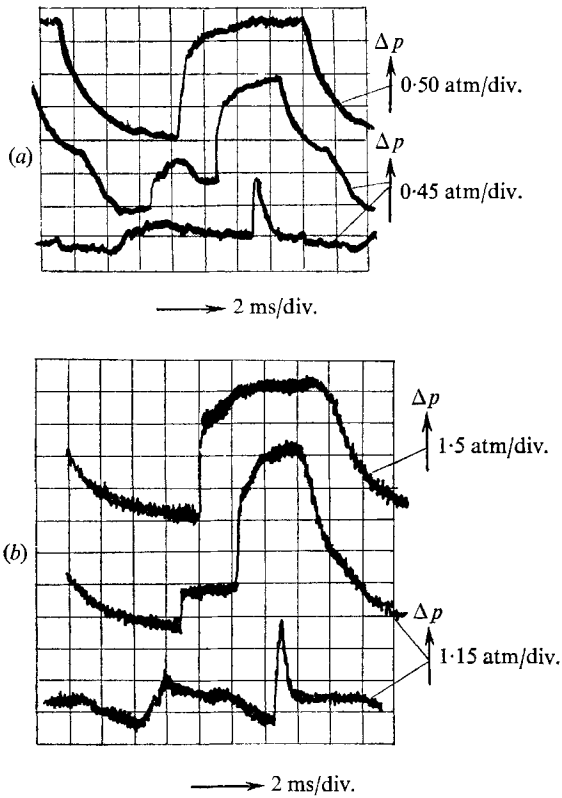


FIGURE 11. Pressure fluctuations at various locations in the resonance tube. (a)  $M_j = 0.8$ ; (b)  $M_j = 2$ . Upper trace, end wall; middle trace, half tube length; lower trace, 20 mm downstream of the tube mouth.

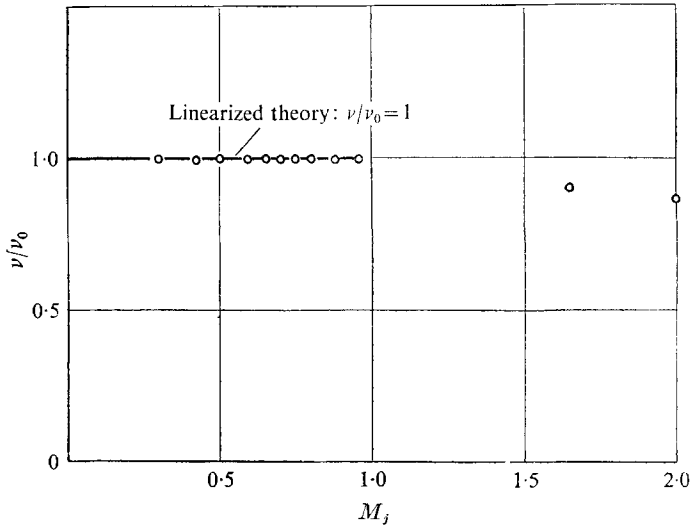


FIGURE 12. Variation of resonance frequency  $\nu$  with jet Mach number.  $\nu_0$  = acoustic frequency of tube.  $\circ$ , experimental points.

The ratio  $\nu/\nu_0$  is plotted on figure 12. It is seen that the result of the linearized theory is excellently verified for  $M_j < 1$ . For  $M_j > 1$ , the frequency decreases slightly.

## 5. Conclusions

The fluid dynamics of the resonance tube has been explained with the help of a simplified model. It has been shown how the oscillations start and grow to a finite amplitude. This amplitude increases with the jet Mach number and is predicted by the theory over a wide range of jet Mach numbers (0.1 to 2). It has been experimentally demonstrated that the 'wake-producing' cylinder laid along the jet axis, proposed by Brocher & Maresca (1969*a, b*) for subsonic jets, also allows the full oscillation amplitude to be achieved in the case of a correctly expanded supersonic jet. The jet enters the tube at supersonic velocity in the compression phase of the cycle, without noticeable spilling.

Further work is presently being done by the authors on a digital computer to study the flow field in more detail. Also the thermal effects are being investigated in the light of the now well established flow model.

The authors wish to thank the Director of the Institut de Mécanique des Fluides de Marseille, Professeur J. Valensi, for his constant encouragements and the permission to publish this paper. Thanks are also due to Mr Issartier and Mr Guillaume of the I.M.F.M. for their advices on experimental techniques and to Professor Dumitrescu of Institut de Mécanique des Fluides Traian Vuia, of the Academie de la République Socialiste de Roumanie, Bucharest, who provided the authors with the capacitive transducers of his own design.

## Appendix

It has to be shown that the series of points given by the intersection of the compression waves having a slope +1 with the ellipse  $E_2$  tends to the limiting point 2.

Considering a continuous single-valued function  $y = f(x)$ , monotonically decreasing and without inflexion point, as is ellipse  $E_2$  in the first quadrant, it is easy to show that two following points of the series are connected by the relation

$$y_{n+1} + y_n = x_{n+1} - x_n. \quad (\text{A } 1)$$

It follows that:

(a) If  $y_n = 0$ ,  $x_{n+1} - x_n = 0$  since  $f(x)$  is decreasing monotonically. This implies  $y_{n+1} = 0$  and in that case the limit cycle is reached.

(b) If  $y_n > 0$ ,  $(x_{n+1} - x_n) > 0$  since  $f(x)$  is decreasing monotonically and single-valued. This implies  $|y_{n+1}| < y_n$ , or  $|y_{n+1}| < |y_n|$ .

(c) If  $y_n < 0$ , (A 1) may be written as  $y_{n+1} - |y_n| = x_{n+1} - x_n$ . Since  $f(x)$  is decreasing monotonically and single-valued,  $x_{n+1} < x_n$  and  $y_{n+1} < |y_n|$ , or  $|y_{n+1}| < |y_n|$ .

Hence, the cases (b) and (c) may be summarized as  $|y_{n+1}| < |y_n|$ .

It remains to show that  $\lim_{n \rightarrow \infty} |y_n| \rightarrow 0$ . Starting from the first cycle, one has

$$\begin{aligned} y_1 &= x_1, \\ y_2 + y_1 &= x_2 - x_1, \\ y_{n+1} + y_n &= x_{n+1} - x_n. \end{aligned}$$

Summing up both sides of these equations, one gets

$$2 \sum_{k=1}^n y_k = x_{n+1} - y_{n+1}.$$

This may be written as

$$2 \left\{ \sum_{y_k > 0} y_k - \sum_{y_k < 0} |y_k| \right\} = x_{n+1} - y_{n+1}. \quad (\text{A } 2)$$

Since the right-hand side of (A 2) is finite, either the terms of both series tend to zero as  $n \rightarrow \infty$ , or they both tend to a limit different from zero. The absolute value of these two limits would be equal since, as has been shown,  $|y_{n+1}| < |y_n|$ ; this would imply  $(x_{n+1} - x_n) \rightarrow 0$  and, as was discussed above, this is not possible since the  $x$  axis is not an axis of symmetry for the ellipse  $E_2$ . Hence, the terms of the two sums may only tend to zero as  $n \rightarrow \infty$  and this demonstrates that the oscillations will grow up with time and reach the limit cycle 1-2-3-4-1.

#### REFERENCES

- BROCHER, E. & MARESCA, C. 1969a *C.R. Acad. Sci. Paris*, **268**, 749.  
 BROCHER, E. & MARESCA, C. 1969b *J. Mécanique*, **8**, 21.  
 BROCHER, E. & MARESCA, C. & HUSSON, M. H. 1969 National conference on applied mechanics, Bucarest. (To be published in *Revue Roumaine des Sciences Techniques, Série de Mécanique Appliquée*.)  
 DUMITRESCU, L. Z. 1967 Techniques and results of model pressure measurements in shock tubes, 6. *International Shock Tube Symposium*.  
 HARTMANN, J. 1919 *Dan. Mat. Fys. Medd.* **1**.  
 HARTMANN, J. & TRUDSO, E. 1951 *Dan. Mat. Fys. Medd.* no. 10, **26**.  
 MANNING, J. R. 1968 *Trans. ASME, Basic Engng.* D **90**, 231.  
 OERTEL, H. 1966 *Stossröhre*. New York: Springer Verlag.  
 SAVORY, L. E. 1950 *Engineering*, **170**, 99 and 136.  
 SPRENGER, H. 1954 *Mitteilungen aus dem Institut für Aerodynamik*, no. 21, 18.  
 THOMPSON, P. A. 1964 *A.I.A.A. J.* **2**, 1230.  
 VREBALOVICH, T. 1962 *Jet Propulsion Laboratory Technical Report* no. 32, 378.



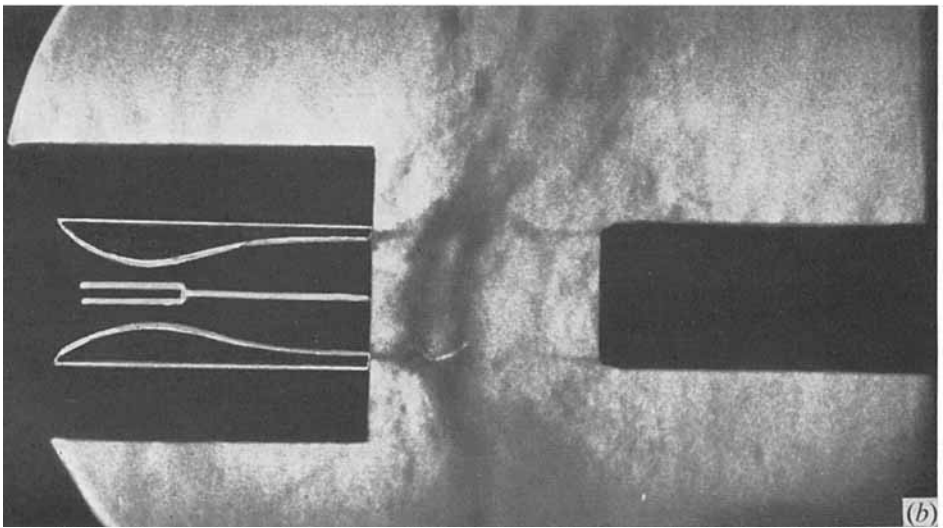
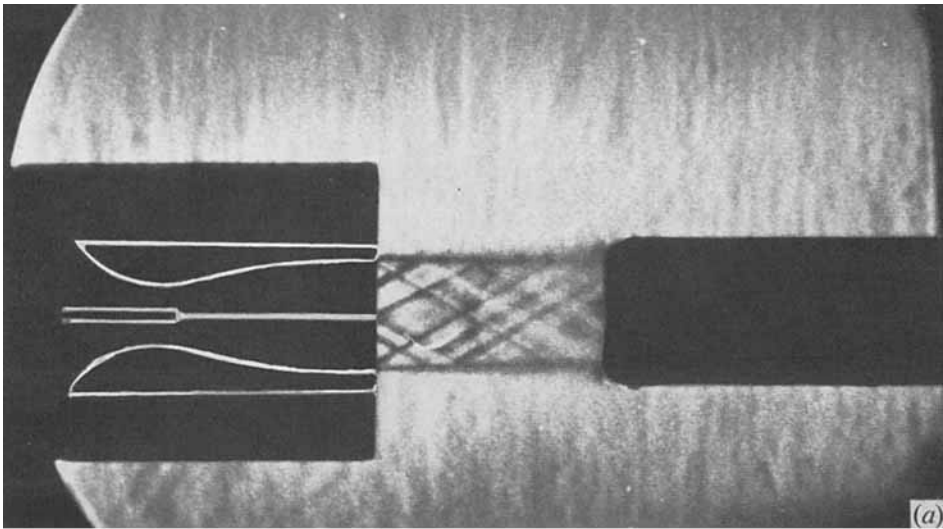


FIGURE 7. Resonance tube excited by a correctly expanded supersonic jet ( $M_1 = 2$ ), with the 'wake-producing' rod. (a) First phase: supersonic penetration of the jet into the tube. (b) Second phase: evacuation of the tube.